Electronic Supplementary Material (ESI) for Analytical Methods.

Supplementary Material

Fluorescent sensor array based on a single cucurbit[5]uril-truxene probe for simultaneous identification of five heavy metal ions

Tingyi Qiao[a], Pei Li[a], Nan Dong[a,b*]

[a]School of Chemistry and Chemical Engineering, Guizhou University, Guiyang, 550025, China

[b]Key Laboratory of Macrocyclic and Supramolecular Chemistry of Guizhou Province, Guiyang, 550025, China

[*]Corresponding author: Tel.:+86 851 83621679; fax: +86 851 83621679
E-mail address: ndong@gzu.edu.cn

1. Synthetic procedures for the cucurbit[5]uril-truxene (Q[5]-Tr) probe

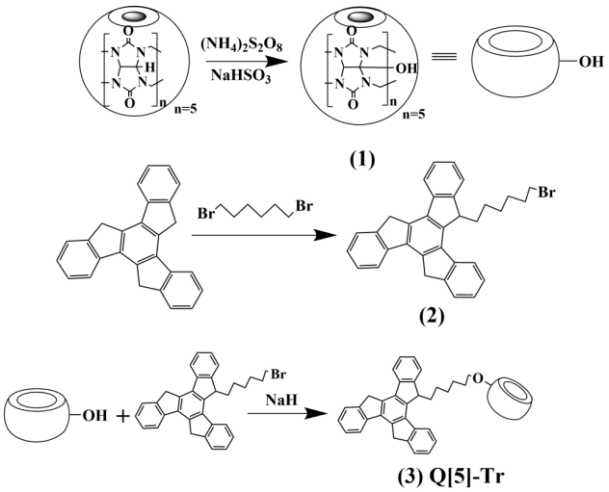

Scheme S1 Synthetic Scheme of Q[5]-Tr.

1.1 Characterization of monohydroxycucurbit[5]uril (1):

^{1}H NMR (400 MHz, D_2O, δ/ppm): 5.57 (d, 8H), 5.50 – 5.30 (m, 10H), 5.18 (s, 1H), 4.44 (d, 2H), 4.20 (dt, 8H). HRMS (*m*/*z*): $[M+K]^+$ calcd. for $C_{30}H_{30}N_{20}O_{11}$, 885.2035 Da; found, 885.2029 Da.

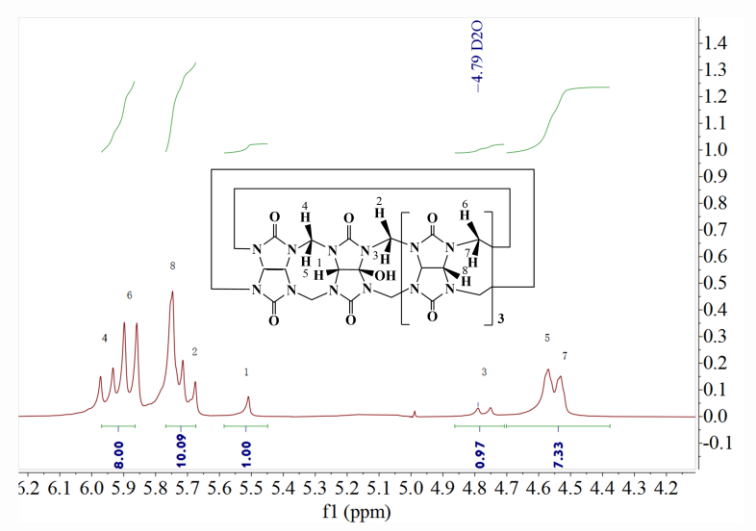

Fig. S1 ^{1}H NMR (400 MHz) of (HO)Q[5] in D_2O

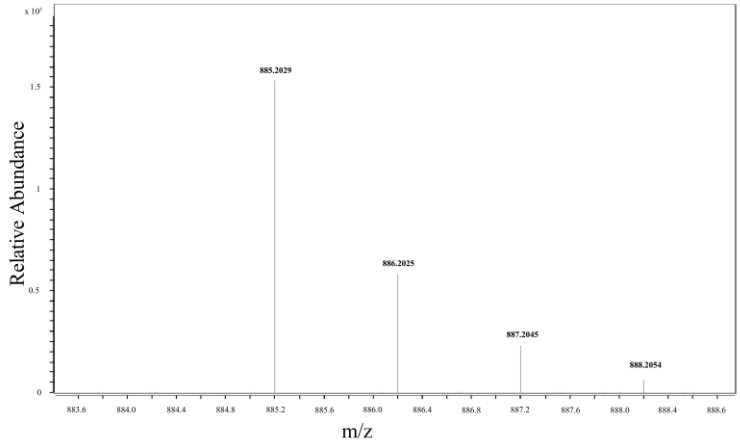

Fig. S2 HRMS (m/s) of (HO)Q[5].

1.2 Characterization of monobromohexyl truxene (2):

^{1}H NMR (400 MHz, $CDCl_3$, δ/ppm): 7.94 (s, 2H), 7.86 (s, 1H), 7.62 – 7.57 (m, 5H), 7.43 (d, 4H), 4.90 – 4.84 (m, 4H), 4.61 (d, 1H), 3.24 (s, 2H), 1.99 (s, 2H), 1.65 (s, 2H), 1.50 (d, 4H), 1.27 (d, 2H). HRMS (*m*/*z*): $[M+H]^+$ calcd. for $C_{33}H_{29}Br$, 425.2269 Da; found, 425.2144 Da.

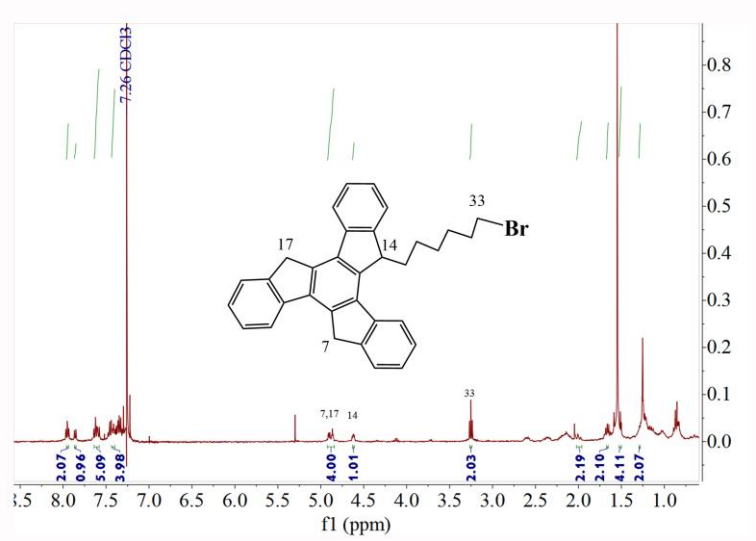

Fig. S3 ^{1}H NMR (400 MHz) of monobromohexyl truxene in $CDCl_3$.

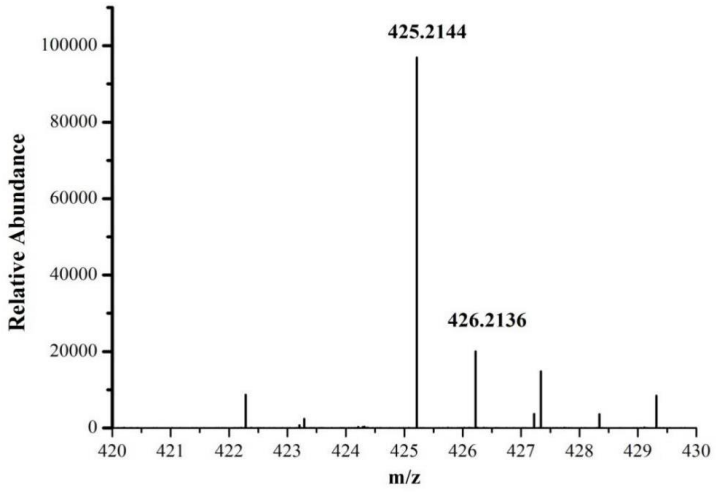

Fig. S4 HRMS (m/s) of monobromohexyl truxene.

1.3 Characterization of Q[5]-Tr (3):

As shown in Fig. S5, we can see the ^{1}H NMR spectroscopy of Q[5]-Tr clearly shows the characteristic peaks belonging to (HO)Q[5] and monobromohexyl truxene. The signal protons (δ=7.46, 7.48, 7.33) were belong to the benzene of monobromohexyl truxene, the signal proton (δ=4.80) was belong to the methylene of monobromohexyl truxene, the signal proton (δ=1.94) was belong to the alkyl chain of monobromohexyl truxene. However, a new signal proton of O–CH_2– (δ=2.64) was masked by the solvent peaks of DMSO-d_6 (δ=3.3, 2.5), which was led to interference with ^{1}H NMR signal protons. And the signal protons (δ=5.55-5.49, 5.33, 4.28) were belong to (HO)Q[5].

Based on the above results, we still can confirm the Q5-Tr was successfully synthesized by means of characteristic peaks belonging to (HO)Q[5] and monobromohexyl truxene.

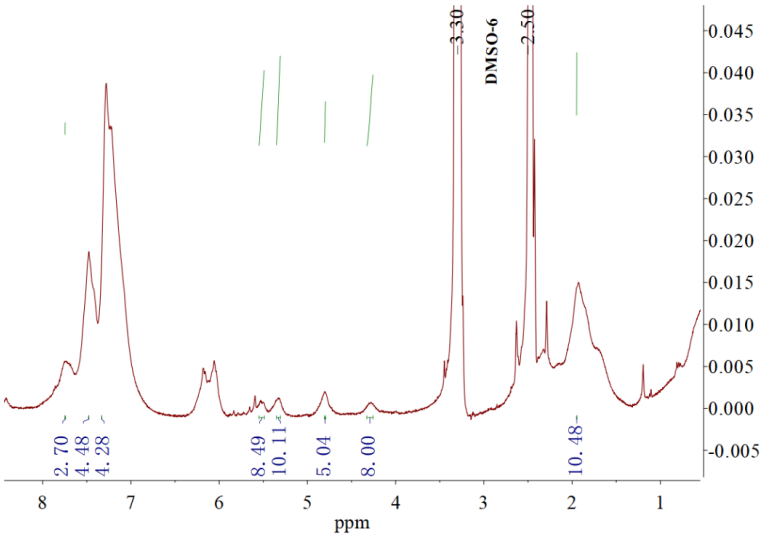

Fig. S5 ^{1}H NMR (400 MHz) of Q[5]-Tr in DMSO-d_6.

2. Purity Analysis of Q[5]-Tr

HPLC of Q[5]-Tr was measured absorption intensity at 296 nm. 10 μL Q[5]-Tr (1.0 μM) in different proportions of the mobile phase (methanol/water) were run at 0.5mL/min for 20min, a peak of LC analysis of Q[5]-Tr manifested the purity (Fig. S6).

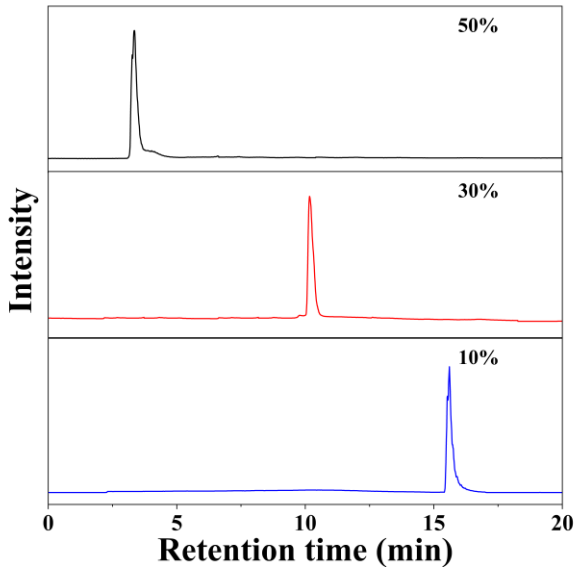

Fig. S6 HPLC analysis of Q[5]-Tr.

3. Option of the pH value of the solution

It was found that the fluorescence intensity of the probe was related to the pH value of the solution (Fig. S7). Under acidic conditions (pH =1.0, 3.0, and 5.0), the

fluorescence intensities were almost same. A similar trend occurred under the two alkaline conditions (pH =8.0 and 9.0). However, the fluorescence intensities of the probe under the acid condition, the alkaline condition and the neutral condition (pH=7.0) were completely different. Moreover, we also detected the fluorescence response of the probe to metal ions in six pH solutions, and the variation of the fluorescence intensity of Q[5]-Tr among the three solutions (pH =3.0, 7.0 and 9.0) were most obvious in Fig. S8, which provided convenience for the construction of the fluorescent sensor array by simply altering the pH of the solution. Based on this, three typical pH solutions (pH =3.0, 7.0, and 9.0) were selected.

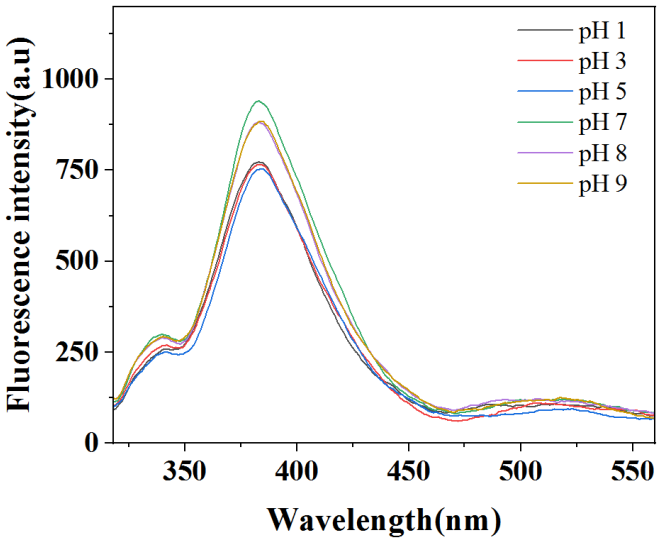

Fig. S7 The fluorescence spectra of Q[5] -Tr (20.0 μM in different pH values solution with 1% DMF).

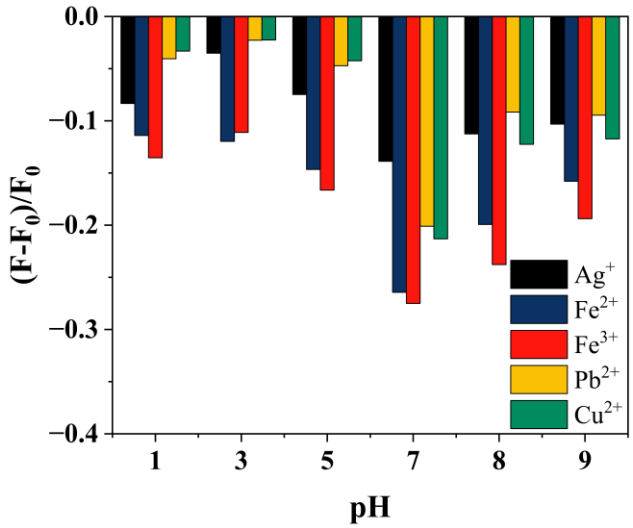

Fig. S8 The fluorescence spectra of Q[5] -Tr to 5 HMIs in different pH value of the solution with 1% DMF).

4. The recognition and classification of the fluorescent sensor array to the HMIs

The Q[5]-Tr sensor array combined with LDA realized the recognition and classification of five different metal ions. As shown in Table S1, the classification accuracy of Q[5]-Tr sensor array towards five HMIs was 100%. Evaluating this model by cross-validation method, classification accuracy was 100%. The recognition and classification of the Q[5]-Tr sensor arrays against five different metal ions (20.0 μM) (Fig. 4A) were same as other concentration of HMIs (10.0 μM, 1.0 μM and 0.1 μM) (Figs. 4B-4D).

Table S1. The recognition and classification of the Q[5]-Tr sensor arrays against five different metal ions (20.0 μM).

Metal			Predicted group membership					
			Ag^{+}	Fe^{2+}	Fe^{3+}	Pb^{2+}	Cu^{2+}	total
Original	count	Ag^{+}	5	0	0	0	0	5
		Fe^{2+}	0	5	0	0	0	5
		Fe^{3+}	0	0	5	0	0	5
		Pb^{2+}	0	0	0	5	0	5
		Cu^{2+}	0	0	0	0	5	5
Cross-validated	count	Ag^{+}	5	0	0	0	0	5
		Fe^{2+}	0	5	0	0	0	5
		Fe^{3+}	0	0	5	0	0	5
		Pb^{2+}	0	0	0	5	0	5
		Cu^{2+}	0	0	0	0	5	5

5. The comparison of LOD of various fluorescent sensor array to the metal ions

The limit of detection (LOD) of the Q[5]-Tr probe-based fluorescent sensing array was taken to be 0.1 μM, which was lower than the published paper. Thus, this suggested that the as-developed sensor array had comparable LOD in metal ions discrimination.

Table S2. Comparison of various fluorescent sensor arrays for the discrimination of different metal ions.

Sensing elements	Type of metal ions	LOD (μM)	Ref.
Copper nanoclusters	12	5	1
bovine serum albumin nanoparticles	18	10	2
Coumarin−Pyridine	7	5	3
Silver nanoclusters	7	3	4
amino acids-modulating quantum dots	9	5	5
Sulfur quantum dots	8	0.5	6
cucurbit[5]uril-truxene	5	0.1	This work

6. The linearity range of the developed sensing system to metal ions

The relationships between EDs and Pb^{2+}, Fe^{3+}, Fe^{2+} and Ag^{+} concentration were examined. Fig. S9 shows that the total Euclidean distance (EDs) versus concentration

curve features a range from 0 to 20.0 μM, and a good linearity range of 0.1-10.0 μM (Fig. S9, inset).

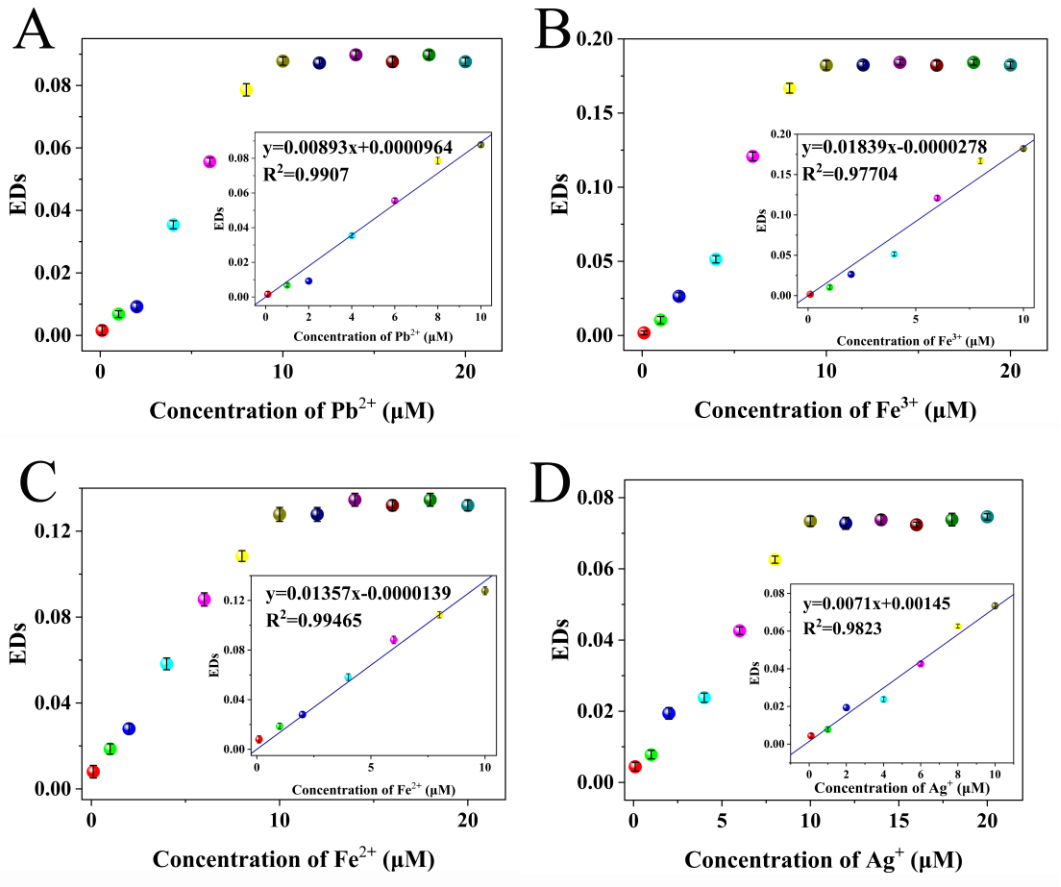

Fig. S9 The EDs score plots of the array to (A) Pb^{2+}, (B) Fe^{3+}, (C) Fe^{2+} and (D) Ag^{+} at various concentrations. Inset respectively shows the linear relationship between the concentrations of four HMIs and their own EDs.

7. The recognition of fluorescent sensor array to the mixture of Cu^{2+} and Pb^{2+}

The data of fluorescent sensor array to the mixture of Cu^{2+} and Pb^{2+} were processed with LDA, which were well separated with 100% identification accuracy. The classification of each metal ions with 100% identification accuracy was confirmed by cross-validation method (Table S3).

Table S3. The recognition and classification of the Q[5]-Tr sensor arrays against the mixture of Cu^{2+} and Pb^{2+} (total concentration of 5.0 μM).

$C_{Cu^{2+}}/C_{Pb^{2+}}$			Predicted group membership							
			1:0	4:1	2:1	1:1	1:2	1:4	0:1	total
Original	count	1:0	5	0	0	0	0	0	0	5
		4:1	0	5	0	0	0	0	0	5
		2:1	0	0	5	0	0	0	0	5
		1:1	0	0	0	5	0	0	0	5
		1:2	0	0	0	0	5	0	0	5
		1:4	0	0	0	0	0	5	0	5
		0:1	0	0	0	0	0	0	5	5
Cross-validated	count	1:0	5	0	0	0	0	0	0	5
		4:1	0	5	0	0	0	0	0	5
		2:1	0	0	5	0	0	0	0	5
		1:1	0	0	0	5	0	0	0	5
		1:2	0	0	0	0	5	0	0	5
		1:4	0	0	0	0	0	5	0	5
		0:1	0	0	0	0	0	0	5	5

8. Discrimination of different HMIs mixtures

Whether our sensor array was sufficient to discriminate the mixtures of different HMIs was explored. The binary HMIs mixtures (Cu^{2+}/Pb^{2+}, Cu^{2+}/Fe^{2+}, Cu^{2+}/Fe^{3+}, Cu^{2+}/Ag^{+}, Pb^{2+}/Fe^{2+}, Pb^{2+}/Fe^{3+}, Pb^{2+}/Ag^{+}, Fe^{2+}/Fe^{3+}, Fe^{2+}/Ag^{+}, Fe^{3+}/Ag^{+}, with a total concentration of 5.0 μM) were well dispersed (Fig. S10A). The discrimination of ternary HMIs mixtures ($Cu^{2+}/Pb^{2+}/Fe^{2+}$, $Cu^{2+}/Pb^{2+}/Fe^{3+}$, $Cu^{2+}/Pb^{2+}/Ag^{+}$, $Cu^{2+}/Fe^{2+}/Fe^{3+}$, $Cu^{2+}/Fe^{2+}/Ag^{+}$, $Cu^{2+}/Fe^{3+}/Ag^{+}$, $Pb^{2+}/Fe^{2+}/Fe^{3+}$, $Pb^{2+}/Fe^{3+}/Ag^{+}$, $Pb^{2+}/Fe^{2+}/Ag^{+}$, $Fe^{2+}/Fe^{3+}/Ag^{+}$, with a total concentration of 5.0 μM) was well dispersed (Fig. S10B). And quaternary HMIs mixtures ($Cu^{2+}/Pb^{2+}/Fe^{2+}/Fe^{3+}$, $Cu^{2+}/Pb^{2+}/Fe^{3+}/Ag^{+}$, $Cu^{2+}/Pb^{2+}/Fe^{2+}/Ag^{+}$, $Cu^{2+}/Fe^{2+}/Fe^{3+}/Ag^{+}$, $Pb^{2+}/Fe^{2+}/Fe^{3+}/Ag^{+}$, with a total concentration of 5.0 μM) also were well separated (Fig. S10C). Through the cross-validation method, this sensor array correctly classified 100% different mixed metal ions (Tables S4-S6).

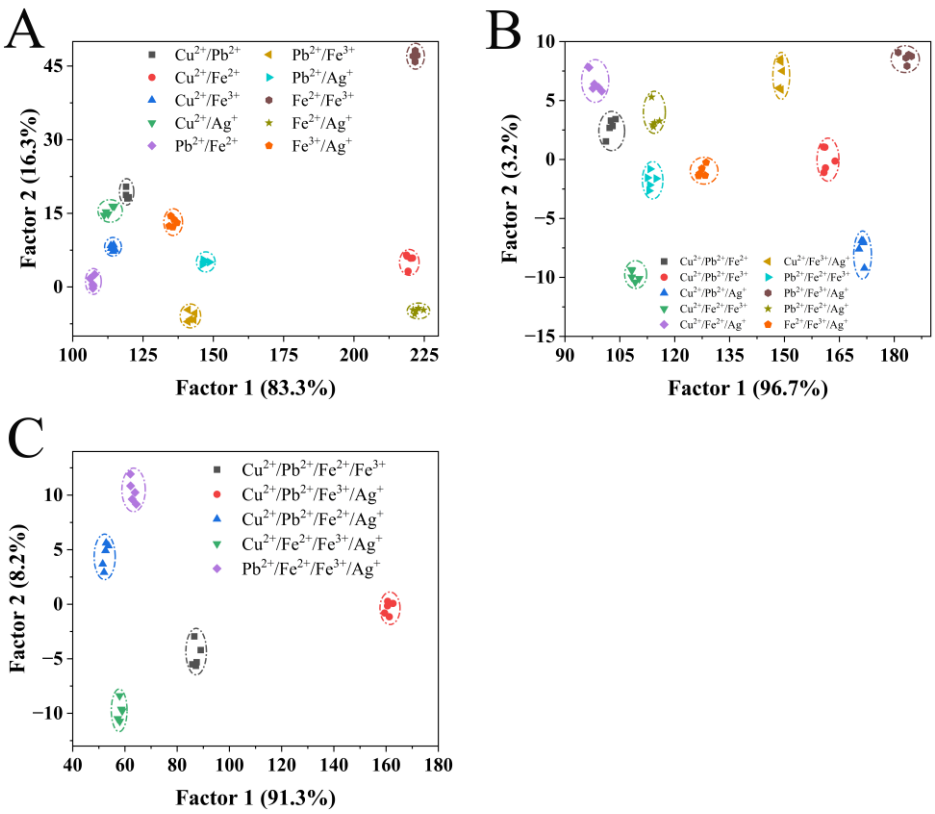

Fig. S10 The canonical score plots for the fluorescence response of the sensor array to discrimination of the mixtures of five HMIs at the total concentration of 5.0 μM.

Table S4. The recognition and classification of the Q[5]-Tr sensor arrays against the binary HMIs mixtures (total concentration of 5.0 μM).

Mixed metal			Predicted group membership										
			1	2	3	4	5	6	7	8	9	10	total
Original	count	1	5	0	0	0	0	0	0	0	0	0	5
		2	0	5	0	0	0	0	0	0	0	0	5
		3	0	0	5	0	0	0	0	0	0	0	5
		4	0	0	0	5	0	0	0	0	0	0	5
		5	0	0	0	0	5	0	0	0	0	0	5
		6	0	0	0	0	0	5	0	0	0	0	5
		7	0	0	0	0	0	0	5	0	0	0	5
		8	0	0	0	0	0	0	0	5	0	0	5
		9	0	0	0	0	0	0	0	0	5	0	5
		10	0	0	0	0	0	0	0	0	0	5	5
Cross-validated	count	1	5	0	0	0	0	0	0	0	0	0	5
		2	0	5	0	0	0	0	0	0	0	0	5
		3	0	0	5	0	0	0	0	0	0	0	5
		4	0	0	0	5	0	0	0	0	0	0	5
		5	0	0	0	0	5	0	0	0	0	0	5
		6	0	0	0	0	0	5	0	0	0	0	5
		7	0	0	0	0	0	0	5	0	0	0	5
		8	0	0	0	0	0	0	0	5	0	0	5
		9	0	0	0	0	0	0	0	0	5	0	5
		10	0	0	0	0	0	0	0	0	0	5	5

Samples marked as 1-10, Cu^{2+}/Pb^{2+}, Cu^{2+}/Fe^{2+}, Cu^{2+}/Fe^{3+}, Cu^{2+}/Ag^{+}, Pb^{2+}/Fe^{2+}, Pb^{2+}/Fe^{3+}, Pb^{2+}/Ag^{+}, Fe^{2+}/Fe^{3+}, Fe^{2+}/Ag^{+}, Fe^{3+}/Ag^{+}.

Table S5. The recognition and classification of the Q[5]-Tr sensor arrays against the ternary HMIs mixtures (total concentration of 5.0 μM).

Mixed metal			Predicted group membership										
			1	2	3	4	5	6	7	8	9	10	total
Original	count	1	5	0	0	0	0	0	0	0	0	0	5
		2	0	5	0	0	0	0	0	0	0	0	5
		3	0	0	5	0	0	0	0	0	0	0	5
		4	0	0	0	5	0	0	0	0	0	0	5
		5	0	0	0	0	5	0	0	0	0	0	5
		6	0	0	0	0	0	5	0	0	0	0	5
		7	0	0	0	0	0	0	5	0	0	0	5
		8	0	0	0	0	0	0	0	5	0	0	5
		9	0	0	0	0	0	0	0	0	5	0	5
		10	0	0	0	0	0	0	0	0	0	5	5
Cross-validated	count	1	5	0	0	0	0	0	0	0	0	0	5
		2	0	5	0	0	0	0	0	0	0	0	5
		3	0	0	5	0	0	0	0	0	0	0	5
		4	0	0	0	5	0	0	0	0	0	0	5
		5	0	0	0	0	5	0	0	0	0	0	5
		6	0	0	0	0	0	5	0	0	0	0	5
		7	0	0	0	0	0	0	5	0	0	0	5
		8	0	0	0	0	0	0	0	5	0	0	5
		9	0	0	0	0	0	0	0	0	5	0	5
		10	0	0	0	0	0	0	0	0	0	5	5

Samples marked as 1-10, $Cu^{2+}/Pb^{2+}/Fe^{2+}$, $Cu^{2+}/Pb^{2+}/Fe^{3+}$, $Cu^{2+}/Pb^{2+}/Ag^{+}$, $Cu^{2+}/Fe^{2+}/Fe^{3+}$, $Cu^{2+}/Fe^{2+}/Ag^{+}$, $Cu^{2+}/Fe^{3+}/Ag^{+}$, $Pb^{2+}/Fe^{2+}/Fe^{3+}$, $Pb^{2+}/Fe^{3+}/Ag^{+}$, $Pb^{2+}/Fe^{2+}/Ag^{+}$, $Fe^{2+}/Fe^{3+}/Ag^{+}$.

Table S6. The recognition and classification of the Q[5]-Tr sensor arrays against the quaternary HMIs mixtures (total concentration of 5.0 μM).

Mixed metals			Predicted group membership					
			1	2	3	4	5	total
Original	count	1	5	0	0	0	0	5
		2	0	5	0	0	0	5
		3	0	0	5	0	0	5
		4	0	0	0	5	0	5
		5	0	0	0	0	5	5
Cross-validated	count	1	5	0	0	0	0	5
		2	0	5	0	0	0	5
		3	0	0	5	0	0	5
		4	0	0	0	5	0	5
		5	0	0	0	0	5	5

Samples marked as 1-5, $Cu^{2+}/Pb^{2+}/Fe^{2+}/Fe^{3+}$, $Cu^{2+}/Pb^{2+}/Fe^{3+}/Ag^{+}$, $Cu^{2+}/Pb^{2+}/Fe^{2+}/Ag^{+}$, $Cu^{2+}/Fe^{2+}/Fe^{3+}/Ag^{+}$, $Pb^{2+}/Fe^{2+}/Fe^{3+}/Ag^{+}$.

9. The possible interaction mechanism

As shown in Fig. S11, the UV visible absorption spectra of the monobromohexyl truxene, (HO)Q[5], and Q[5]-Tr probe interacting with five metal ions. After the addition of metal ions, the UV visible absorption spectra of the monobromohexyl truxene and monobromohexyl truxene - metal ions system indicated that monobromohexyl truxene does not interact with these metal ions (Fig. S11A). Similarly, no change in UV visible absorption was observed for the system of (HO)Q[5]-metal ions because (HO)Q[5] has no UV visible absorption itself (Fig. S11B). Only the UV visible absorption of the Q[5]-Tr system changed after the addition of metal ions (Fig. S11C).

^{1}H NMR was used to investigate the interactions between (HO)Q[5] and Ag^+, Pb^{2+}, Cu^{2+} and the corresponding spectrum shown in Figure S12. When (HO)Q[5] interacted with Ag^+, Pb^{2+}, Cu^{2+}, the chemical shift of Ha, Hb and Hc protons of (HO)Q[5] all moved to the low field. The carbonyl groups of (HO)Q[5] may interact with metal ions through ion-dipole, and cause the change of electron cloud density of proton. The electron cloud density of proton was reduced, which resulted proton shifted to a low field. We did not test the ^{1}H NMR spectra of (HO)Q[5] and Fe^{2+}, Fe^{3+}, because iron ions would destroy the instrument. The experimental result indicated (HO)Q[5] interact with metal ions[7-10].

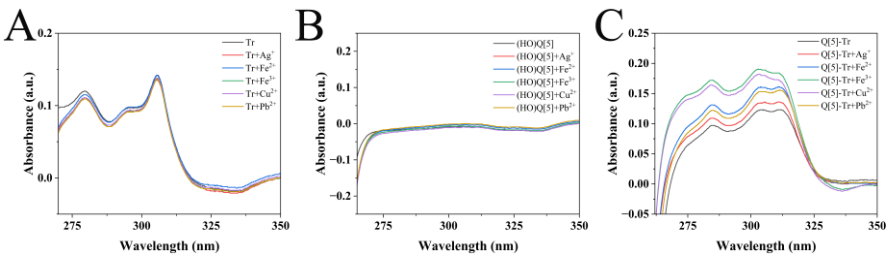

Figure S11. The UV visible absorption spectra of (A) monobromohexyl truxene, (B) (HO)Q[5] and (C) Q[5]-Tr incubated with five HMIs (20.0 μM) respectively.

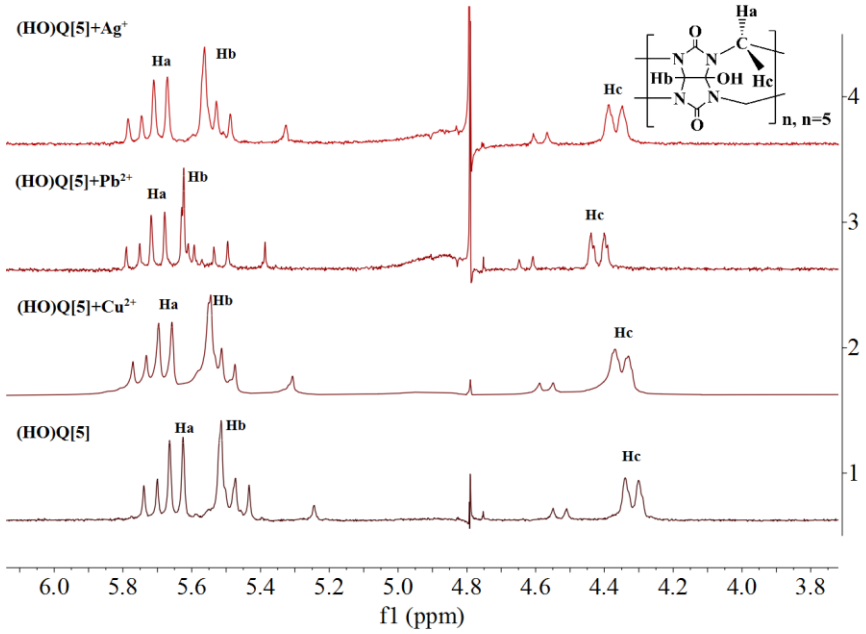

Figure S12. ^{1}H NMR spectra of (HO)Q[5] after addition of metal ions (n_{ions} : $n_{(HO)Q[5]}$ =1:1) in D_2O.(metal ions: Cu^{2+}, Pb^{2+}, Ag^{+})

10. Determination of binding constants

To calculate the binding constant (*K*), the different concentration of heavy metal ions were added to Q[5]-Tr probe solution (3.5 mL 10.0 μM) respectively, the fluorescence intensities of the mixture at 382 nm were recorded.

Based on the method reported in the literature[9,10], the formation of 1:1 complexes between the Q[5]-Tr as well as the HMIs (Scheme S2), the relevant equilibrium constant was defined by eqn (1), where *K* is the association constant of the HMIs with

the Q[5]-Tr, [H], [G] and [HG] are the concentration of the individual species.

$$\mathbf{H + G} \overset{K}{\rightleftharpoons} \mathbf{HG}$$

Scheme S2. The simple 1:1 system.

$$K = \frac{[HG]}{[H][G]} \tag{1}$$

According to the law of mass conservation the concentrations can be expressed as follows, where $[G_0]$ is the total HMIs concentration and $[H_0]$ is the total Q[5]-Tr concentration:

$$[G]_0 = [G] + [HG] \tag{2}$$

$$[H_0] = [H] + [HG] \tag{3}$$

We rearrange eqn (2) and (3) to isolate for [H] and [G], respectively, and insert these into eqn (1) to expand it in the form of eqn (4). Expanding the right-hand denominator to give eqn (5).

$$K = \frac{[HG]}{([H_0] - [HL])([G_0] - [G])} \tag{4}$$

$$K = \frac{[HG]}{([H_0][G_0] - [HL])([H_0] + [G_0] + [HG]^2)} \tag{5}$$

Then rearranging yields the quadratic eqn (6) and the corresponding solution in eqn (7).

$$[HG]^2 - [HG]([H_0] + [G_0] + \frac{1}{K}) - [H_0][G_0] = 0 \tag{6}$$

$$[HG] = \frac{1}{2}([H_0] + [G_0] + \frac{1}{K}) - \sqrt{([H_0] + [G_0] + \frac{1}{K})^2 + 4[\mathrm{H_0}][\mathrm{G_0}]} \tag{7}$$

The equ (8) was revealed the changes in fluorescence intensity of complex up on fluorescence titration, where ΔF is the variation of fluorescence intensity of complex

of Q[5]-Tr and HMIs, Δk is the change in the proportionality constant between the complex and the free Q[5]-Tr.

$$\Delta F = \Delta k[HG] \tag{8}$$

Substituted with eqn (7).

$$\Delta F = \Delta k \frac{([H_0]+[G_0]+\frac{1}{K}) - \sqrt{([H_0]+[G_0]+\frac{1}{K})^2 + 4[H_0][G_0]}}{2} \tag{9}$$

The fluorescence data were analyzed using nonlinear fitting analysis by eqn (9) using Kgraph 4.02, and the nonlinear relationship between $[G_0]/[H_0]$ and ΔF were shown in Fig S13, where m2 represented binding constant (K), where R^2 represented square of correlation coefficient. And the results of the K of the Q[5]-Tr probe to the five HMIs in pH 3.0, 7.0 and 9.0 solutions were listed in Table S7. (M^{n+} represents Ag^+, Fe^{2+}, Fe^{3+}, Pb^{2+} and Cu^{2+})

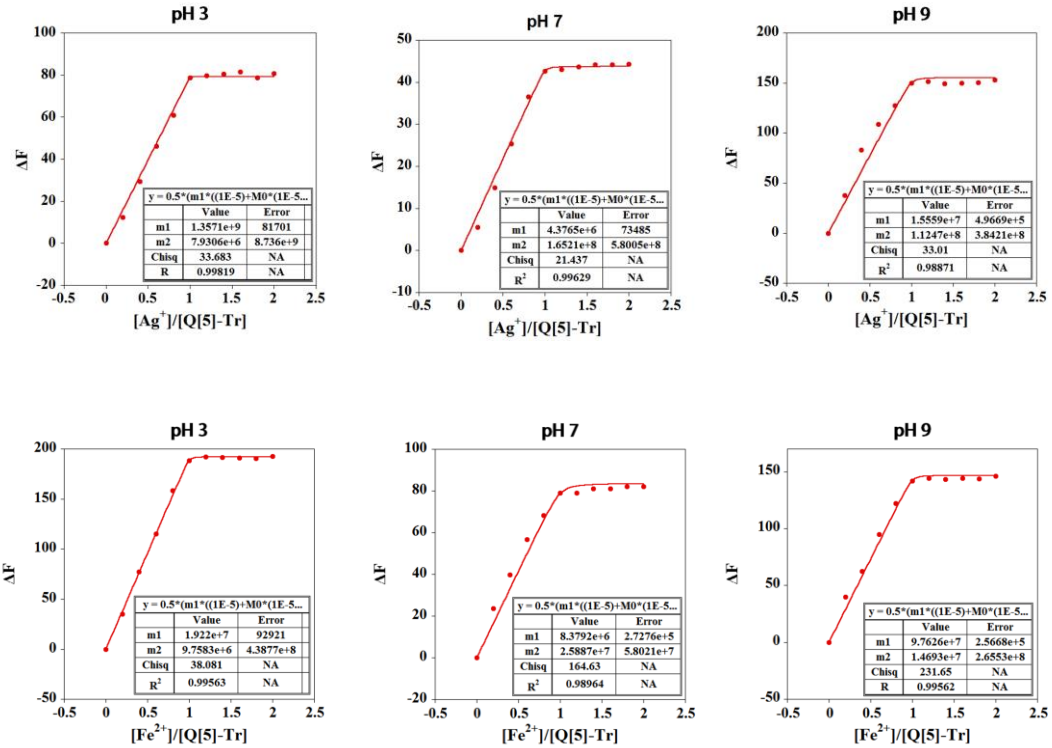

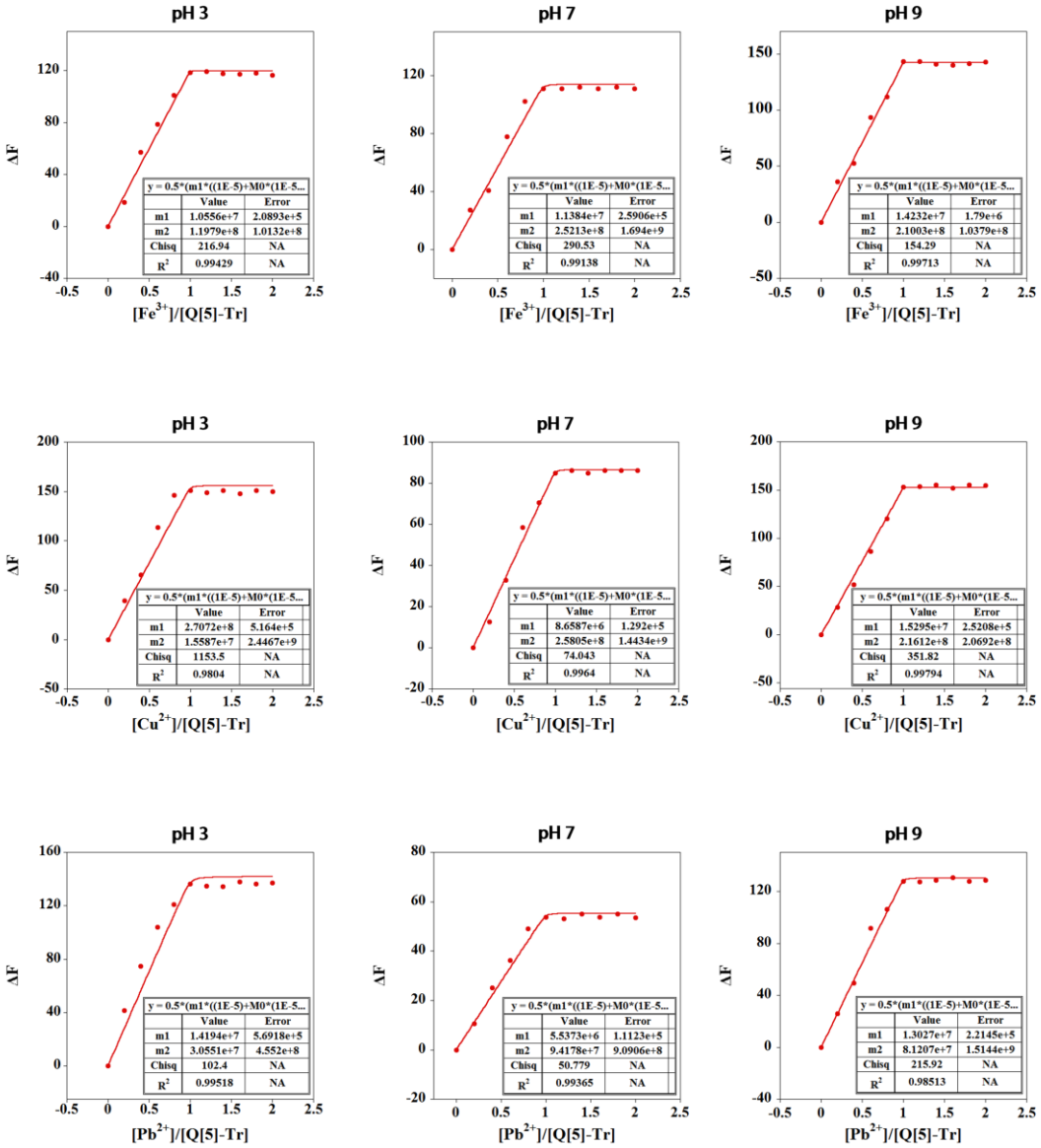

Figure S13. The nonlinear fitting of fluorescence titration between Q[5]-Tr and five HMIs.

Table S7 The binding constants of Q[5]-Tr to five HMIs at different pH solutions.

pH		3		7		9	
		K (L/mol)	R^2	*K* (L/mol)	R^2	*K* (L/mol)	R^2
HMI	Ag^+	7.93×10^7	0.9981	1.65×10^8	0.9963	1.12×10^8	0.9887
	Fe^{2+}	9.76×10^6	0.9956	2.58×10^7	0.9896	1.45×10^7	0.9845
	Fe^{3+}	1.20×10^8	0.9943	2.52×10^8	0.9914	2.10×10^8	0.9971
	Pb^{2+}	3.06×10^7	0.9952	9.42×10^7	0.9937	8.12×10^7	0.9851
	Cu^{2+}	1.56×10^7	0.9804	2.58×10^8	0.9964	2.16×10^8	0.9979

11. Analysis of tap water and lake water

The Q[5]-Tr sensor array combined with LDA realized the recognition and classification of five different metal ions in real simples. As shown in Table S8, the classification accuracy of Q[5]-Tr sensor array towards five HMIs was 100%. Evaluating this model by cross-validation method, classification accuracy was 100%. The recognition and classification of the Q[5]-Tr sensor arrays against five different metal ions (20.0 μM) in tap water were same as lake water.

Table S8. The recognition and classification of the Q[5]-Tr sensor arrays against five different metal ions (20.0 μM) in tap water.

Metal			**Predicted group membership**					
			Ag^+	Fe^{2+}	Fe^{3+}	Pb^{2+}	Cu^{2+}	total
Original	count	Ag^+	5	0	0	0	0	5
		Fe^{2+}	0	5	0	0	0	5
		Fe^{3+}	0	0	5	0	0	5
		Pb^{2+}	0	0	0	5	0	5
		Cu^{2+}	0	0	0	0	5	5
Cross-validated	count	Ag^+	5	0	0	0	0	5
		Fe^{2+}	0	5	0	0	0	5
		Fe^{3+}	0	0	5	0	0	5
		Pb^{2+}	0	0	0	5	0	5
		Cu^{2+}	0	0	0	0	5	5

References:

1 Xu, J., Zhou, H., Zhang, Y., Zhao, Y., Yuan, H., He, X., Wu, Y., Zhang, S., *J. Hazard. Mater.*, 2022, **428**, 128158.

2 Fan, Y.L., Lu, Y.F., Ding, X.Y., Wang, N.H., Xu, F., Shi, G., Zhang, M., *Analyst* ,2020, **145**, 6222-6226.

3 Cao, Z., Li, W., Wan, H., Zhou, J., Jia, X., Ding, Y., *Anal. Chem.*,2021, **93**, 14256-14262.

4 Cao, N., Xu, J., Zhou, H., Zhao, Y., Xu, J., Li, J., Zhang, S., *Microchem. J.*,2020, **159**, 105406.

5 Jing, W., Lu, Y., Yang, G., Wang, F., He, L., Liu, Y., *Anal. Chim. Acta.*,2017, **985**, 175-182.

6 Sun, Z., Xing, H.H., Qing, M., Shi, Y., Ling, Y., Li, N.B., Luo, H.Q., *Chem. Eng. J.*, 2023, **452**, 139594.

7 Ni, X. L., Xue, S. F., Tao, Z., Zhu, Q. J., Lindoy, L.F., Wei, G., *Coordin. Chem. Rev.*, 2015, **287**, 89-113.

8 Ni, X.L., Xiao, X., Cong, H., Liang, L.L., Cheng, K., Cheng, X.J., Ji, N.N., Zhu, Q.J., Xue, S.F., Tao, Z., *Chem. Soc. Rev.*, 2013, **42**, 9480-9508.

9 S. Zhang, L. Grimm, Z. Miskolczy, L. Biczok, F. Biedermann, W.M. Nau, *Chem. Commun.*, 2019, **55**, 14131-14134.

10 R. L. Lin, J. X. Liu, K. Chen, C. Redshaw, *Inorg. Chem. Front.*, 2020, **7**, 3217-3246.

11 P. Thordarson, *Chem. Soc. Rev.*, 2011, **40**, 1305-1323.